AJNR Am J Neuroradiol 25:77–83, January 2004

A Computer-Generated Stereotactic "Virtual Subdural Grid" to Guide Resective Epilepsy Surgery

Kevin Morris, Terence J. O'Brien, Mark J. Cook, Michael Murphy, and Stephen C. Bowden

BACKGROUND AND PURPOSE: **In selected patients undergoing epilepsy surgery, subdural electrode grids play an important role in localizing the epileptogenic zone and identifying eloquent cortex. Determining the relationship of the electrodes to underlying brain architecture traditionally has been difficult. This report describes and validates the use of an original computer-aided method that displays a representation of the electrode positions, based on postimplantation CT or MR findings, coregistered with a 3D-rendered image of the brain, on an image-guided surgery system.**

METHODS: **Seventeen patients underwent the procedure with visual verification of the actual and virtual grids undertaken during the second (postimplantation) surgery. The accuracy of the Virtual Grid electrode positions was further studied in a subgroup of five patients during surgery by plotting the distance from the actual electrode positions by using an infrared stereotactic probe.**

RESULTS: **The accuracy of the Virtual Grid electrode positions by visual inspection was satisfactory in all 17 cases. In the five cases in which quantitative measurements were performed, the mean error for the CT derived electrode positions was 3.4 mm (range 0.5–5.4) compared with the mean error for the MR-derived electrode positions of 2.5 mm (range 0.5–5.2).**

CONCLUSION: **The Virtual Grid electrode positions were highly accurate in localizing the actual position of the subdural electrodes with both CT- and MR-derived images. The MR-derived electrodes demonstrated a trend toward better accuracy, but the CT images were quicker and easier to process. This technology has the potential to minimize both human and technical errors, allowing for a more precise tailoring of the cortical resection in epilepsy surgery.**

The purpose of the presurgical evaluation for intractable partial epilepsy is to define, as precisely as possible, the anatomic location and extent of the epileptogenic zone and, where appropriate, its relationship to the eloquent cortex, in particular primary speech and motor areas. For many years, most epilepsy centers considered the use of intracranial electroencephalography (EEG) recordings a necessary part of the presurgical evaluation (1). The advent of modern neuroimaging has diminished the need for diagnostic intracranial procedures and recordings as it has become clear that noninvasive evaluations are sufficient in most patients in whom a potentially epileptogenic lesion is detected at MR imaging (2). Nevertheless, intracranial recordings still have an important role in presurgical evaluation, particularly when there is very large epileptogenic lesion or where a lesion is adjacent to eloquent cortex exists. A surgically implanted subdural grid over the region of planned resection allows the ictal onset zone to be more precisely localized and also enables functional electrical stimulation mapping of the eloquent cortex to be performed (1).

Before the development of modern imaging techniques the site and extent of intracranial electrode implantations were guided primarily by scalp EEG recordings and clinical features. Scalp EEG has a relatively poor spatial resolution and is often poorly localizing, particularly in extratemporal seizures. The epileptogenic zone may consequently appear to be very extensive and either missing or incorrectly defining the ictal onset zone is a risk, resulting in increased morbidity and reduced chance of success (1, 3, 4). The development of modern neuroimaging techniques, in particular high-resolution MR imaging, positron emission tomography and single photon emission CT, has allowed more targeted implantations to be performed, especially when a stereotactic image guided surgery system (IGSS) is used (5).

The clinical value of subdural electrodes can be

Received March 17, 2003; accepted July 7.

From the Victorian Epilepsy Centre, the Centre for Clinical Neurosciences and Neurological Research, and the Departments of Medicine and Surgery, The University of Melbourne, St. Vincent's Hospital Melbourne, Victoria, Australia.

Address correspondence to M. A. Murphy, Centre for Clinical Neurosciences and Neurological Research, St. Vincent's Hospital, 41 Victoria Parade, Fitzroy, 3065, Victoria, Australia.

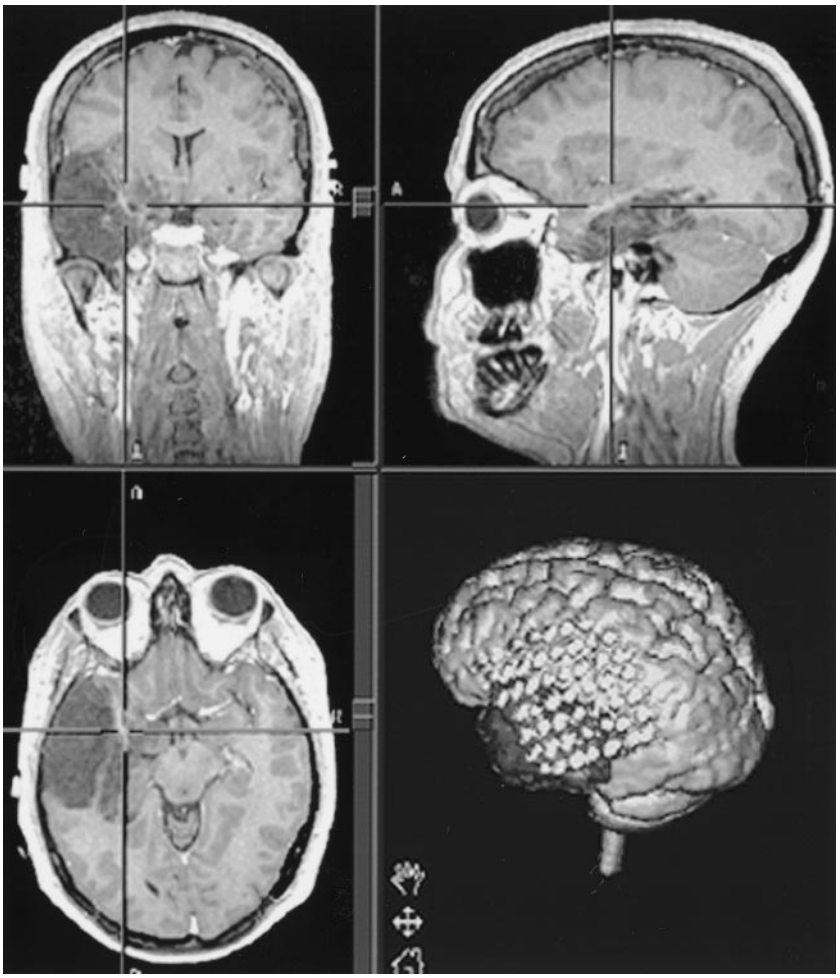

FIG 1. Patient 1. Stereotactic IGSS display shows orthogonal MR imaging views, 3D rendering of segmented brain, lesion, and the Virtual Grid prepared by using a coregistered CT scan.

further enhanced by postimplantation coregistration and 3D visualization of the electrode positions in relation to the cortical surface on the structural or intraoperative MR image. This allows a more precise understanding of the anatomic relationships between the ictal onset zone, eloquent cortex, and underlying brain anatomy. Because the subdural electrodes need to be removed before the cortical resection, the physical relationship of the individual electrode positions on the cortical surface is lost before resection. The site over which the electrodes lie has traditionally been marked by the surgeon manually placing small pieces of numbered paper under the electrodes at the time of their removal. The precise positioning of these markers may be difficult intraoperatively and they may be displaced during the operation. Furthermore, this method does not allow for any movement of the subdural electrodes that may have occurred as a result of the second craniotomy.

In an attempt to improve the utility of subdural electrodes, we have developed an original system that allows the accurate integration and 3D visualization of the position of subdural electrodes (the "Virtual Grid") within an MR-based frameless stereotactic IGSS (Fig 1). The Virtual Grid allows the electrode positions to be precisely identified throughout the operation, even after they have physically been removed from the brain.

The purpose of this report is twofold: first, to describe the technique to implement the system and validate its accuracy and, second, to compare the use of MR imaging and CT for the coregistration of the postimplantation electrode positions.

Methods

Seventeen patients with longstanding medically refractory partial epilepsy underwent subdural grid implantation between May 1999 and December 2002. Over this period, the equipment and software used were subject to normal upgrades, but no significant changes in method were made.

The subdural electrodes were commercially manufactured (Ad-Tech, Racine, WI) and consisted of circular (1-mm height, 4-mm diameter) metal contacts embedded in a thin (0.5-mm) flexible transparent silastic plate and evenly spaced at 10-mm centers. For the first five patients, steel electrode grids were used. For the remaining patients, platinum-iridium grids were used, allowing postimplantation MR images to be acquired. Because these postimplantation MR studies can yield artifacts that obscure electrode positions, CT studies were also acquired as a secondary data source for electrode segmentation.

Subdural electrode implantations were performed with patients under general anesthesia, with the aid of a frameless, infrared, stereotactic surgical navigation system (Stealth Station Image Guided Surgery System, Sofamor Danek, Memphis,

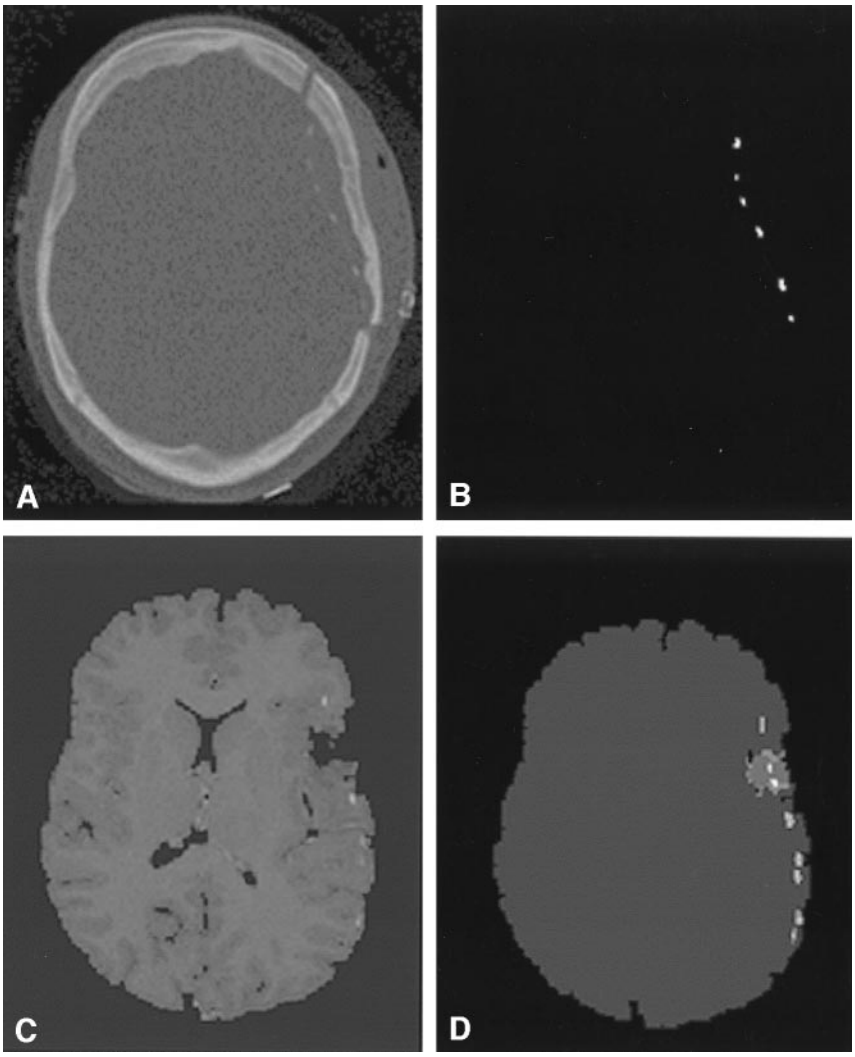

FIG 2. Development of a Virtual Grid by segmentation and co-registration of a post-implantation CT scan.

A, Axial section from the spiral CT scan of the head acquired following implantation of the subdural grid.

B, Binary image of the subdural electrodes that had been segmented from the spiral CT image.

C and *D,* Binary image of the subdural electrode positions (*C*)transformed and combined with the segmented MR image, trileveled image (*D*) representing, respectively, the brain, the lesion, and the subdural electrodes.

TN). For this, a preoperative volumetric MR image (1.0-mm contiguous sections ([1.5-T Vision Magnetom; Seimens, Erlangen, Germany]) was acquired with 10 external fiduciary markers applied to the scalp. Before the commencement of the surgery, the head was fixed in a Mayfield head fixation system (OMI Surgical Products, Cincinnati, OH) and an infrared probe was used to relate the positions of the markers on the scalp to their positions on the MR image from which a transformational matrix was calculated.

The purpose of the implantation was to identify the ictal onset zone and its relationship to eloquent cortical areas more precisely. After recovery from the procedure, patients were returned to the ward for prolonged monitoring by using a 64-channel digital video-EEG machine. Before the second resective surgical procedure, analysis of the epileptogenic zone was done by conducting functional electrical stimulation studies for language and movement.

Five patients were selected over this period for quantitative validation of the accuracy of the Virtual Grid electrodes compared with their actual position during the second surgery. These validating measurements were not applied to consecutive patients. Performing a craniotomy while the patient is awake imposes tight time constraints, and it was left to the neurosurgeon (M.M.) to decide whether there was time to map the actual electrode positions onto the IGSS in each case. In some cases, the neurologist's (M.J.C.) desire to map functional responses from electrocortical stimulation took precedence. Mapping for validation purposes was discontinued once satisfactory validation results had been obtained.

In patient 1, stainless steel subdural grid electrodes were used and a postimplantation CT scan was used to derive the electrode position, which was coregistered to the preimplantation MR image. In patient 2, platinum-iridium electrodes were used and a postimplantation MR imaging volume was used for both the electrode segmentation and as the base volume. In patients 3, 4, and 5, the electrodes were also platinum-iridium, but the Virtual Grid electrodes were segmented from both a postimplantation CT scan and the postimplantation MR imaging volume so that the accuracy of the Virtual Grid electrode positions shown by CT and MR could be directly compared.

Construction and Validation of the "Virtual Grid"

After implantation surgery, a spiral CT scan (Somatom Plus 4; Siemens, Erlangen, Germany) was acquired with 3-mm contiguous cuts through the whole brain, (Fig 2A). Following the switch to platinum-iridium markers, another MR imaging study with fiducial markers was acquired before the resective (second) surgery. The CT and MR imaging images were then transferred to an off-line Unix-based Silicon Graphics work station for the postacquisition processing and registration, which was performed with the aid of commercial image analysis software packages (ANALYZE™ version 7.5 and, subsequently, Analyze/AVW version 4.0, Biomedical Imaging Resource, Mayo Foundation, Rochester, MN).

The construction of the Virtual Grid consisted of three major steps: electrode segmentation (from a postimplantation CT or MR image), registration and transformation of elec-

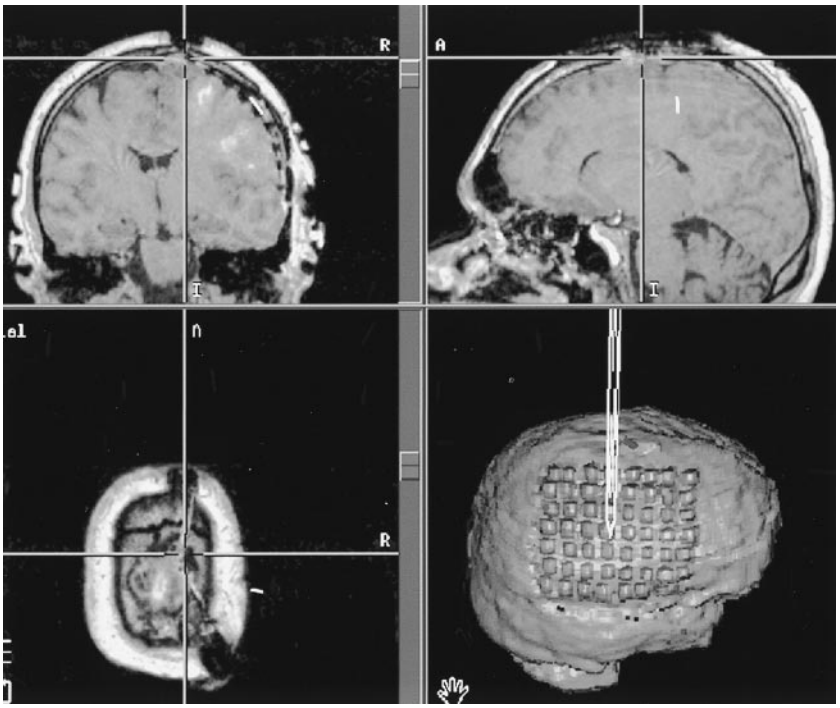

FIG 3. Patient 2. Image-guided surgery system display shows orthogonal MR views, 3D rendering of segmented brain, and subdural grid (prepared by using segmentation of electrodes from the postgrid-implantation MR image).

trodes into the 3D space of the volumetric MR imaging (performed by using the Analyze package), and importation into the stereotactic surgical navigation system.

1. Electrode Segmentation. The electrode positions were segmented from the CT images (patients 1, 3, 4, and 5) by using a threshold-based automatic tracing tool with the seed manually identifying each electrode. On the postimplantation stereotactic MR images, platinum subdural electrodes were segmented by using the same threshold-based technique. The segmented electrodes were then converted into binary format (Fig 2B). Segmentation of electrodes on the MR images (patients 2–5) (Fig 3) was more difficult, requiring greater manual intervention than with that the CT scans because of metal artifact from the wires connecting the electrodes. The smaller section thickness for the MR images (1 mm versus 3 mm) resulted in less volume averaging effect and electrode sizes that were closer to their actual size (compare Figs 1 and 3). In addition, because MR-derived electrode positions were already in the same space as that of the stereotactic MR imaging acquisition to be used during surgery, errors introduced by the CT-MR coregistration were avoided.

2. Registration and Transformation of CT-Derived Subdural Electrodes to 3D Volumetric MR Imaging. This stage was only necessary for the electrodes that were derived from the CT images. Brain was segmented from the extracerebral structures on the CT brain surface by using a semiautomated tracing tool. Segmentation of the brain on the stereotactic MR images was done by using an automated morphologic segmentation tool (Object Extractor, Analyze/AVW version 4.0). The CT and MR imaging–derived segmented brains were then both transformed into binary images, and the CT registered to the MR image by using a Chamfer distance-based surface matching technique, which sampled 1000 points on the surface of both binary images (6). From this a transformation matrix was determined and applied to the CT-based electrode images to transform them into the 3D space of the base stereotactic MR image (Fig 2C).

3. Visualization of Virtual Grid in Stereotactic Surgical Navigation System. A multileveled intensity image was created by adding the MR imaging binary of the brain and the transformed segmented electrodes. Where indicated, a segmented object map of any adjacent lesion was prepared and added to the multilevel image (Fig 2D). This image was then imported into the IGSS as a second volume (the original stereotactic MR imaging being the first volume). A 3D model was then built within the IGSS, displaying the cerebral brain surface, the lesion (where present), and the electrodes as different colored objects with varying levels of transparency (Fig 1).

Comparative Difficulty of MR and CT Segmentation Methods

A virtual grid was produced and used during surgery in all cases. Where the grid of electrodes was placed on a reasonably flat area of cortex, it was straightforward to segment them from either MR imaging or CT volumes. However, in one case, the grid of electrodes was cut into three sections. One section was folded along and beneath the temporal lobe, and another was folded around the occipital lobe and partly slid between the hemispheres. Depth electrodes were also inserted in the mesial temporal lobe of each hemisphere. In this case, it was not possible to produce a clear segmentation of the electrode positions in the short time available when using the postimplantation MR imaging volume. The actual position of many electrodes was obscured by the electrode wires, folded electrode images, and the depth electrodes. The clearer edge and signal intensity definition of electrodes in the CT postimplantation volume produced an accurate and clear result that was used in surgery. For this reason, we always acquire a CT postimplantation scan.

Second Surgery and Use of the Virtual Grid

Approximately 1 week after the subdural grid implantations, the patients returned to the operating room for removal of the grid and the resection of the lesion (if present) and the ictal onset zone. For patient 1, anatomic surface landmarks were used for registration of the IGSS with the preoperative stereotactic MR imaging. For patients 2–5 (with platinum-iridium electrodes), the registration was performed by using new fiducial markers that had been placed on the patient's skull and the second (postimplantation) MR image. Following registration, the opacity of the skull rendering is set to zero and 3D models of the brain, lesion, and grids were built and assigned different

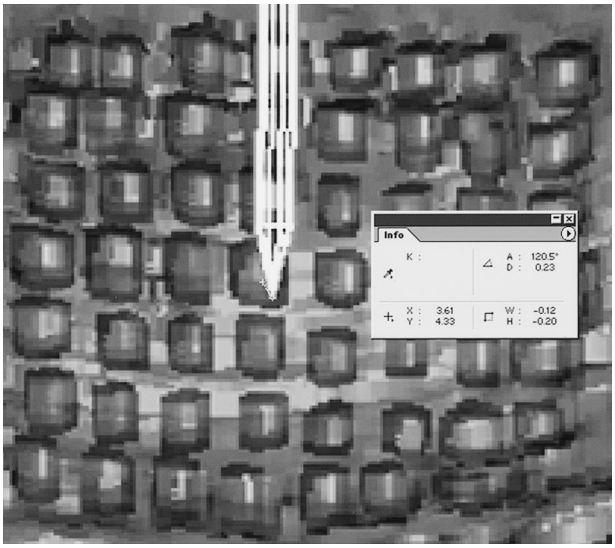

FIG 4. Patient 2. Measuring the displacement of the segmented (MR imaging source) Virtual Grid electrode from the displayed position of the surgeon's infrared probe centered on the actual subdural grid electrode. The image was captured as a "snapshot" and resized so that nearby electrode centers were close to 1 cm apart. The displacement error has been measured as 0.23 cm.

colors. The opacity of the brain is set to 30%, allowing the lesion and grids to be clearly seen on the IGSS 3D rendering (Fig 1).

The wound was then reopened, the bone flap elevated, and the dura opened. The placement of the stereotactic infrared probe on the brain resulted in its corresponding position being displayed in relation to the subdural electrodes in the Virtual Grid and the underlying MR imaging anatomy on orthogonal MR imaging sections as well as on a 3D, multiobject, volume-rendered image (Figs 1 and 3). As a result, the surgeon was able to visualize the position of subdural electrodes in relation to the cortical surface, even after they had physically been removed. In the cases selected for quantitative analysis, the centroids of 10 sample electrodes were registered by using the infrared probe and stored as surgical plans on the IGSS for subsequent validation measurements. The grid was then removed and a volumetric resection was performed incorporating the lesion and electrodes that had been identified as being involved at the ictal onset.

Validation of the Virtual Grid Accuracy

Following surgery, the images and surgical plans were saved digitally by the IGSS. The plans showing the sampled actual electrode positions in the five quantitatively assessed patients were analyzed by manipulating the 3D image of the brain and electrodes so that a surgeon's view of the target electrode was displayed. This corresponds to examining the electrode from directly above and minimizes the radial displacement error observed. The display shows the position of the tip of the infrared probe on the centroid of actual target electrode stored during the craniotomy. To validate the accuracy of the Virtual Grid electrode position, the distance between the tip of the probe and the centroid of the corresponding Virtual Grid electrode was scaled and measured with the Adobe Photoshop measurement tool (Adobe Systems, Inc., San Jose, CA; Fig 4). This procedure was repeated for each of the 10 electrodes sampled for each case.

Results

Virtual Grid Electrode Accuracy

For all 17 patients, qualitative assessment of the accuracy of the Virtual Grid electrode revealed a close match with the actual electrode positions at the second surgery, when the centroid of the electrodes was touched by the infrared problem. The measured errors between the centroid of the Virtual Grid electrodes and that of the actual electrode position at surgery in the five randomly selected patients are given in the Table. The CT-derived Virtual Grid electrodes were displaced by a mean of 3.4 mm (range, 0.5–5.4 mm). The MR-derived Virtual Grid electrodes were displaced by a mean of 2.5 mm (range, 0.5–5.2 mm). The MR-based electrode positions in the three cases (3–5) in which both CT- and MR-based measurements of 10 grid locations were available demonstrated higher accuracy (F [CT, MR imaging] = 49.75; $P = .02$; $\eta^2 = 0.96$) based on the repeated measures analysis of variance. Mauchly's test of sphericity was retained. There was neither significant effect from grid location ($P = .20$) nor significant interaction between image base and grid location ($P = .42$).

Discussion

The clinical utility of any image coregistration–based method, such as the Virtual Grid, is highly dependent on the accuracy of the visualized electrode positions in regard to their true position on the cortical surface. The displacement errors with the Virtual Grid electrodes, compared with that measured with the infrared probe, may be caused by several factors: physical distortion of the cortex during surgery; the effects of partial voluming and section thickness; coregistration errors; and IGSS registration errors.

Physical distortion of the cortex may occur after elevation of the bone flap. The extent of error is dependent on a number of factors, including the underlying disease, patient position, and anesthetic agents used, including diuretics. The presurgical MR image displayed on the IGSS does not reflect these changes; however, because much of this shift is outward radially through the craniotomy, this displacement does not usually result in a significant visual error when viewed from directly above (ie, the surgeon's view).

A partial voluming effect occurs, particularly when 3-mm sections are used in the CT scan of electrodes (Fig 1), which is less pronounced with the MR images acquired with 1-mm-thick sections (Fig 3). This error is also minimized when electrodes are viewed from a perpendicular perspective.

Coregistration errors only occur when the CT scan Virtual Grid electrodes are registered to the preoperative stereotactic MR acquisition. This, combined with the effects of section thickness, likely accounts for the reduced accuracy in CT compared with that of MR-derived electrodes.

IGSS registration errors occur during preoperative

Measured error of the Virtual Grid electrodes as compared with the actual electrode position at the time of surgery determined by a handheld infrared stereotactic probe

Case	Base	Virtual to Actual Electrode Displacement (mm)										Mean	Min	Max
1	CT	3.8	3.5	4.3	3.9	3.4	3.7	3.5	3.7	5.4	3.7	3.89	3.4	5.4
3	CT	0.5	3.6	4.3	3.1	2.3	4.1	3	2.4	4.9	4.2	3.24	0.5	4.9
4	CT	4.3	3.3	3	3.2	4	3.9	4.4	4.2	2.7	2.8	3.58	2.7	4.4
5	CT	2.6	3.8	2.1	2.4	2.7	2.4	2.1	3.3	4.5	2.1	2.8	2.1	4.5
All CT												3.4	0.5	5.4
2	MRI	3	4.1	3.5	2.6	2	1.9	2.7	2.3	1	0.8	2.39	0.8	4.1
3	MRI	0.8	0.5	0.8	1.6	1.3	3	3.2	4.7	4.3	4	2.42	0.5	4.7
4	MRI	1.4	1.4	2.5	2.3	3.5	2.8	5.2	2.6	4.7	3.7	3.01	1.4	5.2
5	MRI	2.9	1.5	1.7	3.3	2.2	1.6	2	1.5	1.8	4.2	2.27	1.5	4.2
All MRI												2.5	0.5	5.2

registration of the stereotactic MR imaging of the patient's head, but standard validation procedures limit these to acceptable levels.

Despite these many potential sources of error, our results show an acceptable degree of accuracy for both the CT- and MR-based Virtual Grid electrodes (Table). The MR-derived Virtual Grid electrodes showed a trend toward greater accuracy as compared with accuracy of CT images; however, segmentation of electrodes from postimplantation MR images was much more difficult and time consuming. In light of a small difference in quantitative accuracy between MR- and CT-derived grids, the practical disadvantages of this method may not justify the increased time and difficulty required. It should be noted, however, that the CT-based method does require the acquisition of an extra image set at additional cost, whereas the MR-based electrode segmentation is performed from the stereotactic images that are acquired just before the second surgery. Our current practice is to acquire a postimplantation CT scan for all patients as a backup for those cases in which the MR imaging segmentation is too difficult to process in the time available.

This technology has the potential to improve postsurgical outcome with respect to seizures while reducing the risk of significant long-term neurologic morbidity. Several studies have shown that, even in patients with discrete neocortical lesions, the chance of rendering the patient seizure-free in the long term is maximized if the ictal onset zone can be completely included in the surgical excision as opposed to performing a simple stereotactic resection of the lesion only (7–10). The technique described in this report minimizes the error in identifying intraoperatively the region of cortex involved in the ictal onset zone. The region of ictal onset usually involves a variable extent of macroscopically normal brain surrounding the epileptogenic lesion and, depending on location, resections of these areas involve the risk of damaging eloquent cortex. To allow a maximal resection of the ictal onset zone to be performed with minimal impact of functional areas, it is essential to use a robust and accurate method of marking the cortical positions over which the subdural electrodes lay.

A previously published study described a surgical navigation system where the position of the subdural electrodes could be registered on the stereotactic MR image at the time of their implantation by manually placing a sterile light-emitting diode rigid probe on each visible electrode (11). These electrode positions are then displayed as disks on the patient's rendered brain surface. Although this is a marked advance over the traditional methods, it does not account for the significant shift in the electrode positions that may occur after the laying of the grid on the brain at the time of replacement of the bone flap and closure of the craniotomy or from the effects of postimplantation bleeding and edema. Our method has the advantage of localizing the electrodes postimplantation when they are in the positions in which the ictal recordings are obtained and functional stimulation studies are performed. In addition, the method described in the earlier report is able to display only the subdural electrodes that were visible within the boundaries of the craniotomy in which our method is able to display all electrodes. This point is particularly important when depth electrodes are used in addition to or instead of subdural electrodes.

Hogan and colleagues (12) reported a method for co-registering postimplantation CT-derived chronic intracranial electrode positions with volumetric MR imaging and single photon emission CT images and state that they were then "integrated into the neurosurgical navigation system"; however, the method by which this second part was achieved was not described, nor was any validation of the accuracy of their methods reported.

Conclusion

The method described and validated here provides an accurate system for mapping subdural electrodes into a Virtual Grid in an IGSS system before the second surgery, thus minimizing operator error and improving outcomes.

References

1. Spencer SS, Sperling MR, Shewmon DA. **Intracranial electrodes.** In: Engel J Jr, Pedley TA, eds. *Epilepsy: A Comprehensive Textbook.* Philadelphia: Lippincott-Raven; 1997:1719–1747
2. Cascino GD, Boon PAJM, Fish DR. **Surgically remediable lesional syndromes.** In: Engel J Jr, ed. *Surgical Treatment of the Epilepsies.* 2nd ed. New York: Raven Press; 1993:77–86

3. Swartz B, Rich J, Dwan P, et al. **The safety and efficacy of chronically implanted subdural electrodes: a prospective study.** *Surg Neurol* 1996;46:87–93
4. Fernandez G, Hufnagel A, Van Roost D, et al. **Safety of intrahippocampal depth electrodes for presurgical evaluation of patients with intractble epilepsy.** *Epilepsia* 1997;38:922–929
5. Murphy MA, O'Brien TJ, Morris KF, Cook MJ. **Multimodality image-guided surgery.** *J Clin Neurosci* 2001;8:534–538
6. Jiang H, Robb R, Holton K. **A new approach to three-dimensional registration of multimodality medical images by surface matching.** *Visualization Biomed Comput* 1992; SPIE The International Society for Optical Engineering 1808:196–213
7. Drake J, Hoffman HJ, Kobayashi J, et al. **Surgical management of children with temporal lobe epilepsy and mass lesions.** *Neurosurgery* 1987;21:792–797
8. Berger MS, Kincaid J, Ojemann GA, et al. **Brain mapping techniques to maximise resection, safety, and seizure control in children with brain tumors.** *Neurosurgery* 1989;25:786–792
9. Yeh HS, Kashiwagi S, Tew JM, Berger TS. **Surgical management of epilepsy associated with cerebral arteriovenous malformations.** *J Neurosurg* 1990;72:216–223
10. Weber JP, Silbergeld DL, Winn HR. **Surgical Resection of epileptogenic cortex associated with structural lesions.** *Neurosurg Clin North Am* 1993;4:327–336
11. Ozlen F, Nakajima S, Chabrerie A, et al. **Excision of cortical dysplasia in the language area with use of a surgical navigator: a case report.** *Epilepsia* 1998;39:1361–1366
12. Hogan RE, Lowe VJ, Bucholz RD. **Triple-Technique (MR imaging, single-photon emission CT, and CT) coregistration for image-guided surgical evaluation of patients with intractable epilepsy.** *AJNR Am J Neuroradiol* 1999;20:1054–1058